PHB)[6,8,28]. Entry vectors were designed to place the gene of interest in an artificial operon with *gfp*. Further details of plasmid construction are available on request.

Dye filling

DiI staining was used to help identify fluorescent neurons in animals that were transgenic for *npr-1::gfp*. Animals were incubated in 10 μg ml^{-1} DiI (Molecular Probes) in M9 Medium for 30 min before examination by confocal microscopy.

Received 24 June; accepted 30 September 2002; doi:10.1038/nature01170.

1. Hodgkin, J. & Doniach, T. Natural variation and copulatory plug formation in *Caenorhabditis elegans*. *Genetics* **146,** 149–164 (1997).
2. de Bono, M. & Bargmann, C. I. Natural variation in a neuropeptide Y receptor homolog modifies social behavior and food response in *C. elegans*. *Cell* **94,** 679–689 (1998).
3. White, J. G., Southgate, E., Thomson, J. N. & Brenner, S. The structure of the nervous system of the nematode *Caenorhabditis elegans*. *Phil. Trans. R Soc. Lond. B* **314,** 1–340 (1986).
4. Wang, Q. & Wadsworth, W. G. The C domain of NETRIN UNC-6 silences calcium/calmodulin-dependent protein kinase- and diacylglycerol-dependent axon branching in *Caenorhabditis elegans*. *J. Neurosci.* **22,** 2274–2282 (2002).
5. Sengupta, P., Chou, J. H. & Bargmann, C. I. *odr-10* encodes a seven transmembrane domain olfactory receptor required for responses to the odorant diacetyl. *Cell* **84,** 899–909 (1996).
6. Dwyer, N. D., Troemel, E. R., Sengupta, P. & Bargmann, C. I. Odorant receptor localization to olfactory cilia is mediated by ODR-4, a novel membrane-associated protein. *Cell* **93,** 455–466 (1998).
7. Stringham, E. G., Dixon, D. K., Jones, D. & Candido, E. P. Temporal and spatial expression patterns of the small heat shock (*hsp16*) genes in transgenic *Caenorhabditis elegans*. *Mol. Biol. Cell* **3,** 221–233 (1992).
8. Yu, S., Avery, L., Baude, E. & Garbers, D. L. Guanylyl cyclase expression in specific sensory neurons: a new family of chemosensory receptors. *Proc. Natl Acad. Sci. USA* **94,** 3384–3387 (1997).
9. Weinshenker, D., Wei, A., Salkoff, L. & Thomas, J. H. Block of an *ether-a-go-go*-like K^+ channel by imipramine rescues *egl-2* excitation defects in *Caenorhabditis elegans*. *J. Neurosci.* **19,** 9831–9840 (1999).
10. Mori, I. Genetics of chemotaxis and thermotaxis in the nematode *Caenorhabditis elegans*. *Annu. Rev. Genet.* **33,** 399–422 (1999).
11. Finn, J. T., Grunwald, M. E. & Yau, K. W. Cyclic nucleotide-gated ion channels: an extended family with diverse functions. *Annu. Rev. Physiol.* **58,** 395–426 (1996).
12. Coburn, C. M. & Bargmann, C. I. A putative cyclic nucleotide-gated channel is required for sensory development and function in *C. elegans*. *Neuron* **17,** 695–706 (1996).
13. Komatsu, H. *et al.* Functional reconstitution of a heteromeric cyclic nucleotide-gated channel of *Caenorhabditis elegans* in cultured cells. *Brain Res.* **821,** 160–168 (1999).
14. Komatsu, H., Mori, I., Rhee, J. S., Akaike, N. & Ohshima, Y. Mutations in a cyclic nucleotide-gated channel lead to abnormal thermosensation and chemosensation in *C. elegans*. *Neuron* **17,** 707–718 (1996).
15. Osborne, K. A. *et al.* Natural behavior polymorphism due to a cGMP-dependent protein kinase of *Drosophila*. *Science* **277,** 834–836 (1997).
16. Ben-Shahar, Y., Robichon, A., Sokolowski, M. B. & Robinson, G. E. Influence of gene action across different time scales on behavior. *Science* **296,** 741–744 (2002).
17. Marsh, D. J., Baraban, S. C., Hollopeter, G. & Palmiter, R. D. Role of the Y5 neuropeptide Y receptor in limbic seizures. *Proc. Natl Acad. Sci. USA* **96,** 13518–13523 (1999).
18. Cowley, M. A. *et al.* Leptin activates anorexigenic POMC neurons through a neural network in the arcuate nucleus. *Nature* **411,** 480–484 (2001).
19. Lee, D. L. & Atkinson, H. J. *Physiology of Nematodes* (Macmillan, London, 1976).
20. Li, C., Nelson, L., Kyuhyung, K., Nathoo, A. & Hart, A. C. Neuropeptide gene families in the nematode *Caenorhabditis elegans*. *Ann. NY Acad. Sci.* **897,** 239–252 (1999).
21. Schwartz, M. W., Woods, S. C., Porte, D. Jr, Seeley, R. J. & Baskin, D. G. Central nervous system control of food intake. *Nature* **404,** 661–671 (2000).
22. Robinson, G. E., Fahrbach, S. E. & Winston, M. L. Insect societies and the molecular biology of social behavior. *Bioessays* **19,** 1099–1108 (1997).
23. Giraldeau, L.-A. & Caraco, T. *Social Foraging Theory* (Princeton Univ. Press, Princeton, New Jersey, 2000).
24. Sulston, J. & Hodgkin, J. *The Nematode Caenorhabditis elegans* (ed. Wood, W. B.) 587–606 (Cold Spring Harbor Laboratory, Cold Spring Harbor, 1988).
25. Clark, S. G., Lu, X. & Horvitz, H. R. The *Caenorhabditis elegans* locus *lin-15*, a negative regulator of a tyrosine kinase signaling pathway, encodes two different proteins. *Genetics* **137,** 987–997 (1994).
26. Mello, C. C., Kramer, J. M., Stinchcomb, D. & Ambros, V. Efficient gene transfer in *C. elegans*: extrachromosomal maintenance and integration of transforming sequences. *EMBO J.* **10,** 3959–3970 (1991).
27. Walhout, A. J. *et al.* GATEWAY recombinational cloning: application to the cloning of large numbers of open reading frames or ORFeomes. *Methods Enzymol.* **328,** 575–592 (2000).
28. Li, C., Kim, K. & Nelson, L. S. FMRFamide-related neuropeptide gene family in *Caenorhabditis elegans*. *Brain Res.* **848,** 26–34 (1999).

Supplementary Information accompanies the paper on *Nature*'s website (http://www.nature.com/nature).

Acknowledgements We thank C. Bargmann, A. Fire, R. Horvitz, C. Li, I. Mori, A. Wei and S. Yu for sharing unpublished data, constructs and strains; T. Stiernagle and the *Caenorhabditis* Genetics Centre for strains; and G. Brown, N. Hopper, N. Tremain and C. Bargmann for suggestions. Some of this work was done while M.d.B. was in the laboratory of C. Bargmann. We are grateful to B. Amos and S. Reichelt for assistance with confocal microscopy.

Competing interests statement The authors declare that they have no competing financial interests.

Correspondence and requests for materials should be addressed to M.d.B. (e-mail: debono@mrc-lmb.cam.ac.uk).

Progenitor cell maintenance requires *numb* and *numblike* during mouse neurogenesis

Petur H. Petersen*†, Kaiyong Zou*†, Joseph K. Hwang*, Yuh Nung Jan‡ & Weimin Zhong*

** Department of Molecular, Cellular and Developmental Biology, Yale University, New Haven, Connecticut 06520, USA*
‡ Howard Hughes Medical Institute and Departments of Physiology and Biochemistry, University of California, San Francisco, California 94143, USA
† These authors contributed equally to this work

Neurons in most regions of the mammalian nervous system are generated over an extended period of time during development. Maintaining sufficient numbers of progenitors over the course of neurogenesis is essential to ensure that neural cells are produced in correct numbers and diverse types[1–3]. The underlying molecular mechanisms, like those governing stem-cell self-renewal in general, remain poorly understood. We report here that mouse *numb* and *numblike* (*Nbl*)[4–6], two highly conserved homologues of *Drosophila numb*[7,8], play redundant but critical roles in maintaining neural progenitor cells during embryogenesis, by allowing their progenies to choose progenitor over neuronal fates. In *Nbl* mutant embryos also conditionally mutant for mouse *numb* in the nervous system, early neurons emerge in the expected spatial and temporal pattern, but at the expense of progenitor cells, leading to a nearly complete depletion of dividing cells shortly after the onset of neurogenesis. Our findings show that a shared molecular mechanism, with mouse Numb and Nbl as key components, governs the self-renewal of all neural progenitor cells, regardless of their lineage or regional identities.

In *Drosophila*, Numb is a membrane-associated signalling protein that allows two daughter cells to adopt different fates after an asymmetric division. It does this by localizing to only one half of the cell membrane in dividing precursor cells, so that it is segregated primarily to one cell[7,8]. On the basis of studies in the developing mouse neocortex, we have postulated that mouse Numb segregates to, and promotes the fate of, progenitor cells in asymmetric divisions that generate a neuron and a daughter progenitor cell during mammalian neurogenesis[4]. This view, however, is controversial; others have postulated instead that vertebrate Numb proteins promote the neuronal fate in such divisions[6,9,10]. *numb* mutant mice exhibit severe defects in cranial neural tube closure and die around embryonic day (E) 11.5, but neurogenesis abnormalities are limited[10,11] and insufficient to resolve the controversy. From studies to be described elsewhere, we generated *Nbl* homozygous mutant mice, which are viable, fertile and exhibit no obvious phenotypes. We find low levels of *Nbl* expression in E8.5 embryos, including in neural progenitor cells. Moreover, embryos mutant for both mouse *numb* and *Nbl* die around E9.5 with more widespread defects than single mutants.

We therefore used Cre-*loxP* mediated gene targeting[12] to examine their function in neurogenesis. We generated a transgenic line (*NesCre8*) with Cre expression controlled by a *nestin* promoter[13] that is active in neural progenitor cells and somites. Within the nervous system, Cre-mediated recombination[14] is readily detectable in a majority of the progenitor cells at E8.5 ($n = 7/9$) and becomes nearly complete by E12.5 (Fig. 1a, and data not shown). Conditional knockout (cKO) using *NesCre8* and a floxed mouse *numb* allele[11] did not cause embryonic lethality or defects in neural tube closure. In fact, cKO mice are viable, fertile and indistinguishable from their wild-type littermates (data not shown). As expected, immunoblots show mouse Numb protein level is already greatly reduced in E9.5 conditional mutant embryos (Fig. 1b). Most of the residual mouse

Numb protein probably comes from tissues where Cre is not active.

Mouse *numb* cKO in the *Nbl* homozygous mutant background (conditional double-knockout, or cDKO), on the other hand, results in embryonic lethality. We never recovered cDKO mice postnatally, whereas those with other allelic combinations, in particular cKO in *Nbl* heterozygous background, are viable and exhibit no gross morphological or behavioural defects. cDKO embryos are indistinguishable from their littermates at E9.5 ($n = 7$), but become completely necrotic by E12.5 ($n = 4$). Those recovered at E11.5 are considerably smaller than the littermates ($n = 8$), suggesting that cDKO embryos die around this stage.

At E10.5, cDKO embryos were consistently recovered (33/183, 1/4 or 1/8 expected). They are 80–90% the size of their wild-type or single-mutant littermates, although many (21/33) are within the range of variation seen in wild-type litters. cDKO embryos are morphologically appropriate for their age with the expected somite numbers, but have significantly reduced telencephalic vesicle (Fig. 1c, right panel) and undulating spinal cord (Fig. 1e, right), the combination of which can be reliably used to identify them. Histological analysis reveals that E10.5 cDKO embryos have severe thinning of the neural tube, from the most rostral telencephalon to caudal spinal cord, including optic discs (Fig. 1d–f, right). In 82% of the mutants, the neuroepithelium is only one-quarter to one-half the thickness of that in the littermates, with frequent buckling of the surface.

E10.5 wild-type neuroepithelium consists mainly of progenitor cells that make up the wider, inner ventricular zone, with a much smaller number of neurons forming the outer mantle zone. We could detect neurons in E10.5 cDKO embryos, in a region-specific pattern similar to that in control littermates, wild-type or other allelic combinations, using two general neuronal markers, anti-HuC/D (Hu; Fig. 2a′–c′, in red) or Neurofilament (NF; Fig. 2d′–g′, in green) ($n = 10$). *Dll1*, a marker for newborn, migrating neurons in the ventricular zone[15,16], is also expressed throughout the cDKO nervous system ($n = 5$) (Fig. 2h′–l′), including the forebrain, which has few Hu- or NF-positive neurons (Fig. 2a′, h′). In fact, the cDKO neuroepithelium frequently contains large patches of *Dll1*-positive cells (Fig. 2i′, l′), unlike in control embryos where they are invariably discrete (Fig. 2i, l).

To assess the severity of the neural progenitor cell loss in E10.5 cDKO embryos, we first used an antibody against phospho-Histone H3 (P-H3) to identify mitotic cells. In wild-type embryos, neural progenitor cells within the neural tube undergo S phase (DNA synthesis) when their nuclei are in the outer half of the ventricular zone. The nuclei then translocate towards the ventricular surface where cells undergo mitosis. Accordingly, P-H3-positive cells form a near continuous outline of the ventricular surface (Fig. 2a–c). In the cDKO nervous system, however, there is a dramatic reduction of P-H3-positive cells (Fig. 2a′–c′). We quantified the loss in the forebrain, the hindbrain (at the level of otic vesicle), and the spinal cord (at cervical levels), which ranges from about 80% to near 100% ($n = 5$).

We next performed bromodeoxyuridine (BrdU) labelling experiments. BrdU is incorporated into DNA by S-phase cells and, therefore, the number of cells labelled during a short pulse reflects the number of cells still proliferating but not in mitosis. There is little variation among control littermates in the pattern and percentage of neural progenitor cells labelled by BrdU (Fig. 2d–g). In forebrain, hindbrain and cervical spinal cord sections, BrdU-labelled cells account for about 49, 33 and 40% of the ventricular zone cells, respectively ($n = 3$; 1-h pulse). In contrast, only a few BrdU-positive cells are present in the cDKO nervous system, indicating a loss of over 99% of the S-phase cells ($n = 14$) (Fig. 2d′–g′).

To confirm that the near-absence of proliferating cells in E10.5 cDKO embryos reflects an absence of neural progenitor cells, rather than their becoming quiescent or defective in cell-cycle progression, we examined the expression of Nestin protein, a commonly used neural progenitor cell marker. Nestin-positive cells are reduced in numbers, but not completely absent, in the E10.5 cDKO neural tube (data not shown). As Nestin is transiently detectable in newborn neurons, probably inherited from progenitor cells, we would expect a more severe reduction at E11.5. This is indeed the case ($n = 3$) (Fig. 2m′, n′). More importantly, loss of Nestin expression is specific to the nervous system; expression in somites in the same cDKO embryos is not affected (Fig. 2n′, arrow).

Because the results with Nestin at E10.5 were inconclusive, we performed *in situ* hybridization using *Hes5*, which marks neural progenitor cells and is essential for keeping them undifferentiated[17]. As expected, there is a sharp reduction of *Hes5* expression in the E10.5 cDKO neuroepithelium ($n = 6$). In the hindbrain, for example, *Hes5*-expressing cells normally occupy two-thirds the width of the neuroepithelium (Fig. 2o). In the cDKO hindbrain, however, there is only a thin layer of scattered *Hes5*-expressing cells near the ventricular surface (Fig. 2o′). Similar loss can be observed in the ventral half of the spinal cord, where *Hes5* is highly expressed in wild-type embryos (Fig. 2p, p′).

We point out that the near-complete absence of neural progenitor cells, as described above, is based on the analysis of, and invariably observed in, embryos with a neural tube that is less than half the normal thickness, a group representing 82% (27/33) of the cDKO embryos we recovered at E10.5. Furthermore, BrdU-labelled cells in

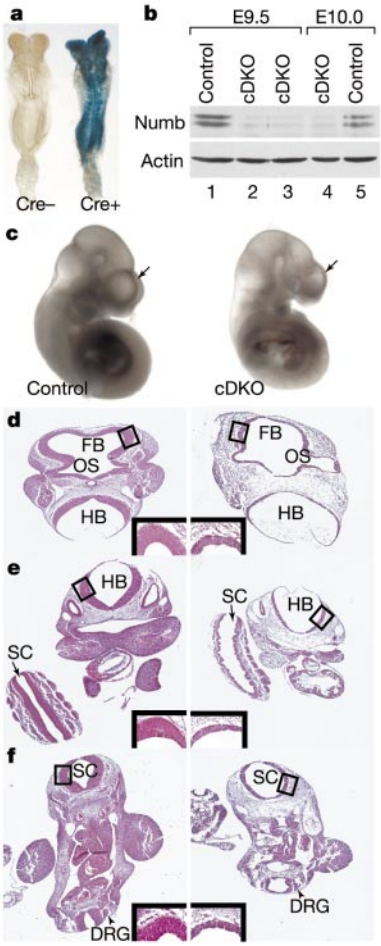

Figure 1 Conditional double knockout of mouse *numb* and *Nbl*. **a**, Cre activity at E8.5 (X-gal staining of *Rosa26* Cre-reporter[14] in *NesCre8*). **b**, Mouse Numb protein level in single embryo extracts from control (1, $Nb^{f/+}$;$Nbl^{-/-}$;*NesCre8*; 5, $Nb^{+/-}$;$Nbl^{-/-}$;*NesCre8*) and cDKO (2–4) (immunoblot). **c**–**f**, left, An E10.5 control littermate ($Nb^{f/+}$; $Nbl^{+/-}$). **c**–**f**, right, An E10.5 cDKO. Sectioning of the cDKO (**c**, right) reveals severe thinning throughout the neural tube (**d**–**f**, right; HE staining). DRG, dorsal root ganglion; FB, forebrain; HB, hindbrain; OS, optic stalk; SC, spinal cord.

many non-neural tissues are also reduced in numbers. Whether this is a secondary effect or shows a direct requirement for mouse *numb* and *Nbl* in non-neural tissues remains to be determined.

What causes the near-absence of neural progenitor cells in E10.5 cDKO embryos? At E9.5, such embryos show no significant defects in cell proliferation (Fig. 4c′ and data not shown; $n = 4$). Consistently, the overall neural tube thickness in E9.5 and E10 cDKO embryos is comparable to that in control littermates ($n = 7$ each), although the mutant neuroepithelium, particularly the ventral spinal cord, is sometimes punctuated by thinner regions. At E10, however, S-phase cells in the nervous system are reduced in numbers (Fig. 3a, b, bottom, and Fig. 4h′), particularly in regions with more active neurogenesis, indicating that the absence of progenitor cells at E10.5 is probably due to defects in self-renewal rather than smaller or defective founding populations. There is, however, significant variation in the severity of such loss among cDKO embryos ($n = 5$), probably due to the perdurance effect of the mouse Numb protein and variations in the onset of Cre expression. Consequently, E10.25 cDKO embryos show varying degrees of neural tube thinning and reduction of BrdU-labelled cells, ranging from a near-complete loss (data not shown) to about 60% (Fig. 3c, f, bottom and inset).

Between E10 and E10.5, mostly neurons are being generated in wild-type embryos. cDKO embryos show no ectopic expression of glia markers like *Sox10* or *Olig2*[18–20], indicating an absence of premature gliogenesis (data not shown). We therefore examined neuron production in E10 and E10.25 cDKO embryos to ascertain whether the inability of neural progenitor cells to self-renew results from their progenies all adopting neuronal fates, which would cause an initial overproduction of neurons and, more importantly, a significant increase of their percentage within the neuroepithelium owing to a depletion of progenitor cells. Other causes, such as progenitor cells becoming quiescent or defective in cell-cycle progression, or undergoing programmed cell death (apoptosis), should affect neuron production negatively, resulting in fewer neurons, both in absolute numbers and as a percentage of the neuroepithelium.

We analysed E10.25 cDKO embryos in which neural tube thinning is not yet apparent ($n = 2$). Three lines of evidence show unambiguously that a diminished self-renewal capability among cDKO neural progenitor cells indeed results from over-differen-

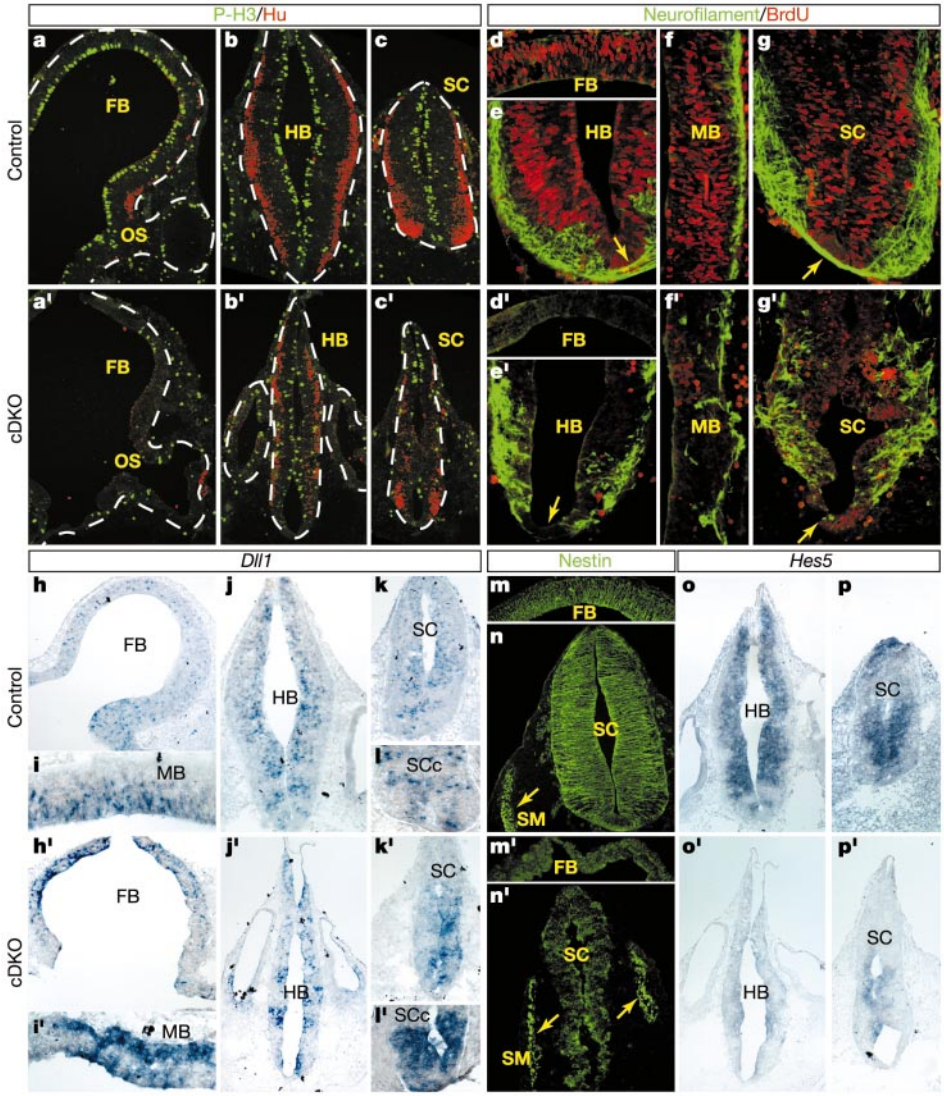

Figure 2 Effect of mouse *numb* and *Nbl* conditional double mutation on neurogenesis. **a**–**p**, Control littermates from E10.5 (**a**–**l**, **o**, **p**; *Nb*$^{f/+}$;*Nbl*$^{+/-}$;*NesCre8*) and E11.5 (**m**, **n**; *Nb*$^{f/+}$;*Nbl*$^{+/-}$). **a**′–**p**′, cDKO embryos from E10.5 (**a**′–**l**′, **o**′, **p**′) and E11.5 (**m**′, **n**′). Absence of neural progenitor cells in the cDKO is evident from the near-absence of mitotic cells (**a**′–**c**′; P-H3 in green), S-phase cells (**d**′–**g**′; BrdU in red), and Nestin (**m**′, **n**′) and *Hes5* (**o**′, **p**′) expression. 10 × magnification except in **d**–**g**, **d**′–**g**′ (25 ×) and **i**, **l**, **i**′, **l**′ (20 ×). FB, forebrain; HB, hindbrain; MB, midbrain; OS, optic stalk; SC and SCc, rostral and caudal spinal cord, respectively; SM, somite.

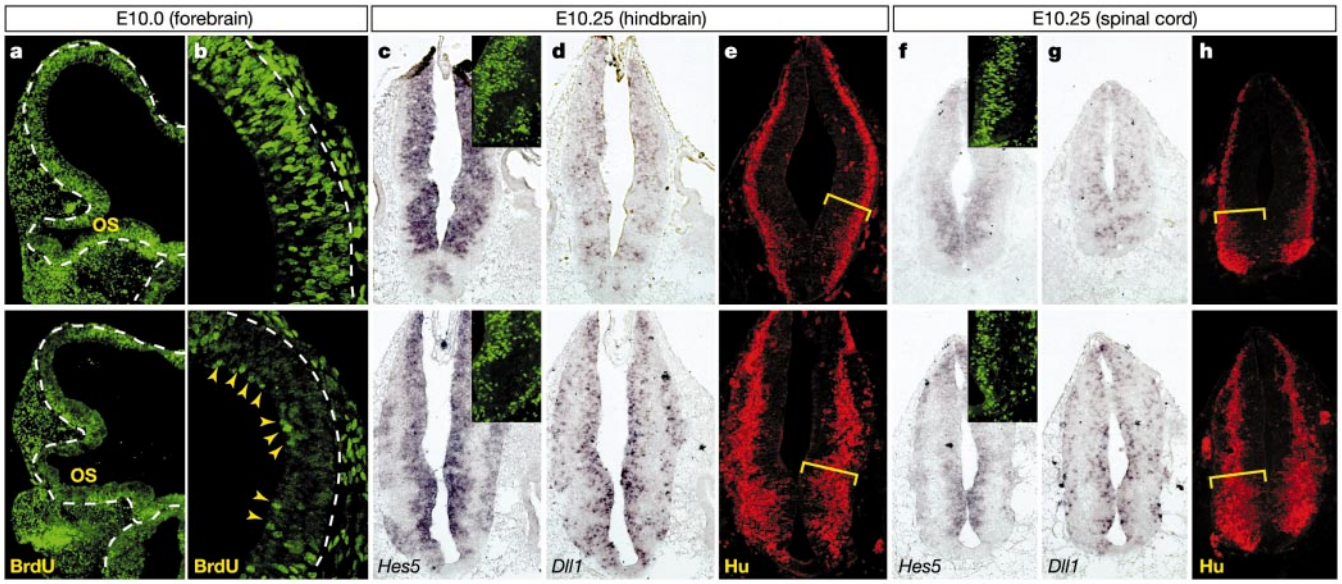

Figure 3 Effect of mouse *numb* and *Nbl* conditional double mutation on neurogenesis before neural tube thinning. **a**–**h**, top, Control littermates from E10.0 (**a**, **b**, top; $Nb^{f/-}$; $Nbl^{+/-}$;*NesCre8*) and E10.25 (**c**–**h**, top; $Nb^{f/+}$;$Nbl^{-/-}$;*NesCre8*). **a**–**h**, bottom, cDKO embryos from E10.0 (**a**, **b**, bottom) and E10.25 (**c**–**h**, bottom). Decreases in progenitor cells (**c**, **f**, bottom; BrdU in green and *Hes5* expression) are accompanied by increases in *Dll1* (**d**, **g**, bottom) and Hu (**e**, **h**, bottom, in red) positive neurons. Arrowheads in **b**, bottom, point to mitotic cells labelled earlier by BrdU. OS, optic stalk. 10 × magnification except in **b**, top and bottom (40 ×).

tiation of their progenies. First, reductions in the number of BrdU-labelled cells are accompanied by a similar decrease in cells expressing progenitor marker *Hes5* (Fig. 3c, f, bottom). Second, within progenitor domains marked by *Hes5*, a higher percentage of cells express *Dll1*, a marker for newborn neurons[15,16] (Fig. 3d, g, bottom; sections are adjacent to those in Fig. 3c, f, bottom, respectively). Third and most important, there is a significant expansion of, proportional to the decrease of progenitor domains, cells expressing neuronal marker Hu (Fig. 3e, h, bottom, and Fig. 5). In these cDKO embryos, there are patches of *Hes5*-positive progenitor cells at the most lateral positions of the neuroepithelium (Fig. 3c, f, bottom). It remains to be determined whether they had migrated aberrantly, or whether their nuclei were physically prevented from translocating medially owing to neuron overproduction near the ventricular surface.

We analysed in more detail neurogenesis in the ventral spinal cord, where motor neurons emerge shortly after E9 and are continuously generated until E13.5. At E9.5 (Fig. 4a–c, a′–c′), cDKO and control embryos ($n = 4$) show little difference in Olig2 and Isl1 expression, which marks motor progenitors and motor neurons, respectively[21–24]. By E10, less than two cell cycles later, there are dramatic differences. At cervical levels in control embryos (Fig. 4d–f), wild-type or other allelic combinations, which are indistinguishable, Isl1-positive neurons colonize the lateral half of the motor domain, whereas Olig2-positive progenitor cells occupy the medial half[21–24]. On average, only 25.6% ($n = 6$ sections from three embryos) of the Olig2-expressing cells are doubly positive for Isl1, representing newborn motor neurons. In contrast, Isl1-expressing cells frequently span the entire width of the cDKO neuroepithelium ($n = 4/5$) (Fig. 4d′–f′, right). As expected, more Olig2-positive cells in the mutant co-express Isl1, ranging from 40.6% to as high as 68.7% (Fig. 4f′, right). Even in regions where motor neurons appear to have only colonized the lateral positions, Olig2-positive cells are also absent from the ventricular zone and many, consistent with their position, co-express Isl1 (Fig. 4d′–f′, left).

Neurogenesis in the spinal cord proceeds in a rostral to caudal gradient. More caudally, there are more Olig2 single-positive cells than that at cervical levels in E10 cDKO embryos. Although the overall reduction of BrdU-labelled cells within the spinal cord is limited, it is much more severe among Olig2-expressing cells, which sometimes show no BrdU incorporation at all (Fig. 4g′–h′, right). Accordingly, in E10.25 cDKO embryos ($n = 2$) at similar caudal levels, Isl1-positive motor neurons span the entire width of the neuroepithelium and most of the remaining Olig2-positive cells co-express Isl1 (Fig. 4i′, j′).

Although neurons are initially overproduced in cDKO embryos, there is significant increase in apoptosis among mutant neurons (Fig. 5, in red), indicating that many die shortly after birth. This is consistent with the absence of axon tracts underneath the floor plate (Fig. 2e′, g′, arrow), and suggests a role for mouse *numb* and *Nbl* in later events of neural development, as we have postulated[5], although neuronal death may be a secondary effect.

It remains possible that cDKO progenitor cells adopt an abnormal developmental pathway and differentiate *en masse* before the onset of neurogenesis. However, two lines of evidence strongly suggest that they are rapidly depleted as neurogenesis progresses because their daughter cells all adopt neuronal fates instead of self-renewing after division. First, in cDKO embryos where BrdU-labelled S-phase cells are significantly reduced in numbers but not totally absent, the number of mitotic cells is comparable to that in control littermates (Fig. 3b, bottom, arrowheads, Fig. 5, P-H3, in blue). Second, whereas neuron overproduction is observed throughout the cDKO nervous system, it is more pronounced in regions where neurogenesis has been more active. In the control E10.25 forebrain, for example, only a few scattered Hu-positive neurons are present (Fig. 5a, left), indicating that neurogenesis was just underway. Neurons are overproduced in the cDKO forebrain, but represent only a small fraction of the neuroepithelium (Fig. 5a, right). On the other hand, ventral spinal cord in control littermates contains large numbers of neurons (Fig. 5e, left). Accordingly, Hu-positive neurons not only are overproduced in the cDKO but also span nearly the entire width of the neuroepithelium (Fig. 5e, right). Similar differences in neuron overproduction can be observed in other regions (Fig. 5b–d, right) and along the dorsoventral neural axis (Fig. 3h, bottom).

The findings reported here are consistent with our earlier hypothesis[4,5], and demonstrate unequivocally that the main function of *numb* homologues in mouse neurogenesis is to maintain progenitor cells, not promoting neuronal fates, during the initial progenitor

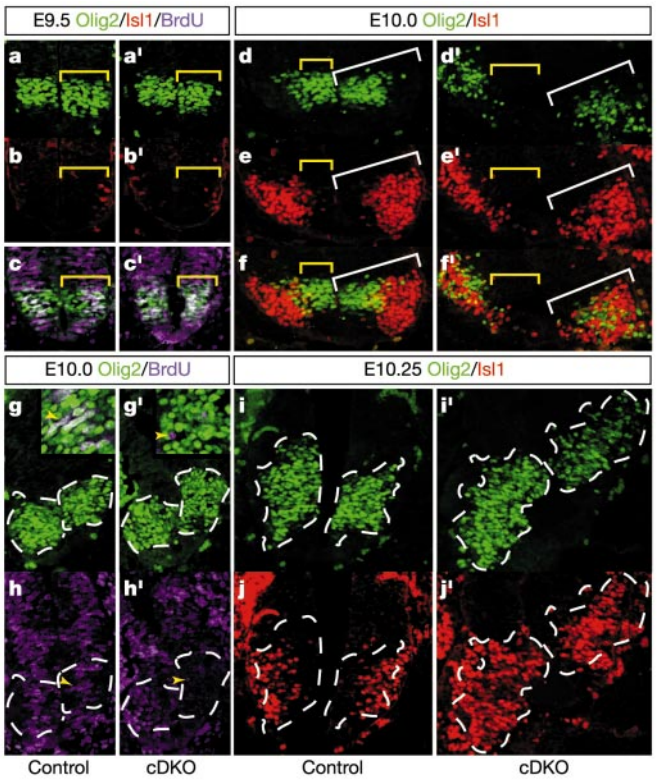

Figure 4 Motor neuron generation at the expense of progenitor cells. **a**–**j**, Control littermates from E9.5 (**a**–**c**; *Nb*$^{f/+}$;*Nbl*$^{+/-}$), E10.0 (**d**–**h**; *Nb*$^{f/+}$;*Nbl*$^{+/-}$;*NesCre8*), and E10.25 (**i**, **j**; *Nb*$^{f/+}$;*Nbl*$^{-/-}$;*NesCre8*). **a**′–**j**′, cDKO embryos from E9.5 (**a**′–**c**′), E10.0 (**d**′–**h**′), and E10.25 (**i**′, **j**′). Cervical (**a**–**f**, **a**′–**f**′) or caudal (**g**–**j**, **g**′–**j**′) spinal cord sections were double-labelled for Olig2 (in green) and Isl1 (in red) or BrdU (in pink). After E9.5, proliferating motor progenitor cells decrease rapidly in numbers in cDKO embryos (**g**′, **h**′). Consistently, cDKO motor neurons often span the entire width of the neuroepithelium (**d**′–**f**′, **i**′, **j**′).

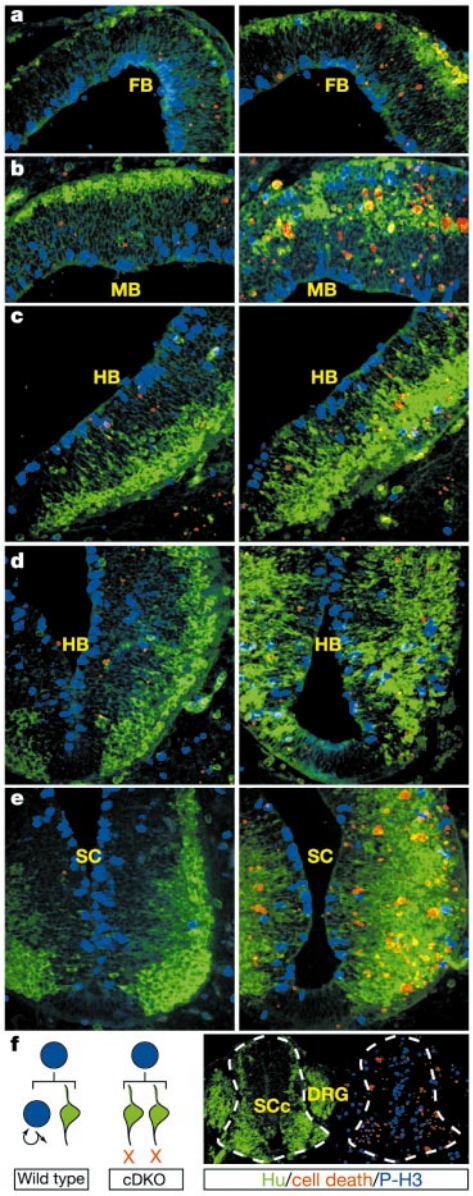

Figure 5 Neuron overproduction and death in mouse *numb* and *Nbl* conditional double-mutant embryos. Compared to the control (**a**–**e**, left), triple labelling reveals that increases in apoptosis (in red) in the cDKO (**a**–**f**, right) are largely confined to regions with Hu-positive neurons (in green). As shown schematically in **f**, left, nervous system phenotypes in cDKO mutants probably result from both daughters of neural progenitor cells (blue filled circle) adopting neuronal fates (in green) and then undergoing apoptosis (red X). Embryos (E10.25) are the same as in Fig. 3. Magnification in **f**, right, is two-fifths of that in parts **a**–**e**. DRG, dorsal root ganglion; FB, forebrain; HB, hindbrain; MB, midbrain; SC and SCc, rostral and caudal spinal cord, respectively. HB sections in **c**, left and right, are rostral to those in **d**, left and right, respectively.

versus neuronal fate decision. This is also supported by gain-of-function studies in chick showing an increase in progenitors among neuroepithelial cells over-expressing chick Numb[9]. A near-absence of motor and sensory neurons in mouse *numb* single mutants at E10.5 due to impaired differentiation has been reported[10]. This phenotype is not seen in our single or cDKO mutants and, therefore, is unlikely to be due to a loss of mouse *numb* function.

Our findings are, to our knowledge, the first direct evidence of a pan-neural program for precursor cells, regardless of their lineage or regional identities, to choose between proliferation and differentiation. There is growing evidence from direct imaging experiments that asymmetric cell division occurs during mammalian neurogenesis[25–27]. Mouse Numb is asymmetrically localized to the apical membrane in dividing progenitor cells[4,5,28], but how Nbl protein is distributed in these cells is unknown, owing to low levels of expression. Therefore, although an effect on asymmetric division can account for pan-neural progenitor depletion in cDKO embryos (Fig. 5f, left), further studies are necessary to ascertain this, in particular the specific effects on multipotential neural stem cells and progenitors with more limited developmental potentials. Similarly, to ascertain if mouse Numb and Nbl act by inhibiting Notch activity like *Drosophila* Numb, it is necessary to determine first whether Notch signalling plays a generic role in regulating cell fate choices between proliferation and differentiation—as seen with mouse Numb and Nbl—or acts differently in different progenitor populations.

Finally, the widespread defects exhibited by mouse *numb* and *Nbl* constitutive double mutants at E9.5 raise an interesting possibility that these two genes are involved in stem-cell self-renewal in other tissues. If mouse Numb and Nbl proteins indeed act like their *Drosophila* counterpart, they would provide an attractive molecular mechanism to integrate lineage or cell-extrinsic cues for progenies of various stem cells to choose between self-renewal and adopting appropriate differentiated fates. □

Methods

Generation of mutant mice

The *Nbl* null (−) allele, lacking 90% of the coding region, was generated using homologous recombination in ES cells and will be described elsewhere. The floxed (f) and

null (also named Δ5,6) alleles of mouse *numb* were generated previously[11]. The *NesCre8* transgene was constructed by inserting a Cre complementary DNA with a nuclear localization signal and chick *β-actin* poly-adenylation site (a gift from M. Lewandoski) immediately 3′ to the *nestin* transcription start site in a vector with 5.8 kilobases (kb) of upstream promoter and 3.2 kb of downstream sequence, including the first two introns[13] (a gift from U. Lendahl). Transgenic mice were produced as previously described[29]. cDKO embryos were generated by mating $numb^{f/f}$;$Nbl^{-/-}$ males with $numb^{+/-}$;$Nbl^{+/-}$;*NesCre8* females. The latter were either hemizygous or homozygous for the *Cre* transgene.

Histology and embryo staining

X-gal staining, immunoblot, immunostaining, BrdU labelling, and *in situ* hybridization were as previously described with minor modifications[4,5,11,29]. Anti-Actin, BrdU (Sigma), HuC/D (Molecular Probes), Isl1 and Nestin (Developmental Studies Hybridoma Bank) are mouse monoclonal, whereas anti-NF (m_r 150K, Chemicon), Olig2 (a gift from H. Takebayashi) and P-H3 (Upstate Biotechnology) are rabbit polyclonal. Apoptosis was detected using a kit (Roche). Probes for *Dll1* and *Hes5* are based on mouse and rat cDNAs, respectively.

Received 18 June; accepted 23 August 2002; doi:10.1038/nature01124.

1. Anderson, D. A. Stem cells and pattern formation in the nervous system: the possible versus the actual. *Neuron* **30,** 19–35 (2001).
2. Edlund, T. & Jessell, T. M. Progression from extrinsic to intrinsic signaling in cell fate specification: a view from the nervous system. *Cell* **96,** 211–224 (1999).
3. McConnell, S. K. Constructing the cerebral cortex: neurogenesis and fate determination. *Neuron* **15,** 761–768 (1995).
4. Zhong, W., Feder, J. N., Jiang, M.-M., Jan, L. Y. & Jan, Y. N. Asymmetric localization of a mammalian Numb homolog during mouse cortical neurogenesis. *Neuron* **17,** 43–53 (1996).
5. Zhong, W., Jiang, M.-M., Weinmaster, G., Jan, L. Y. & Jan, Y. N. Differential expression of mammalian Numb, Numblike and Notch1 suggests distinct roles during mouse cortical neurogenesis. *Development* **124,** 1887–1897 (1997).
6. Verdi, J. M. *et al.* Mammalian NUMB is an evolutionarily conserved signaling adapter protein that specifies cell fate. *Curr. Biol.* **6,** 113–145 (1996).
7. Rhyu, M. S., Jan, L. Y. & Jan, Y. N. Asymmetric distribution of numb protein during division of the sensory organ precursor cell confers distinct fates to daughter cells. *Cell* **76,** 477–491 (1994).
8. Spana, E. P., Kopczynski, C., Goodman, C. S. & Doe, C. Q. Asymmetric localization of numb autonomously determines sibling neuron identity in the *Drosophila* CNS. *Development* **121,** 3489–3494 (1995).
9. Wakamatsu, Y., Maynard, T. M., Jones, S. U. & Weston, J. A. NUMB localizes in the basal cortex of mitotic avian neuroepithelial cells and modulates neuronal differentiation by binding to NOTCH-1. *Neuron* **23,** 71–81 (1999).
10. Zilian, O. *et al.* Multiple roles of mouse *numb* in tuning developmental cell fates. *Curr. Biol.* **11,** 494–501 (2001).
11. Zhong, W. *et al.* Mouse *numb* is an essential gene involved in cortical neurogenesis. *Proc. Natl Acad. Sci. USA* **97,** 6844–6849 (2000).
12. Gu, M., Marth, J. D., Orban, P. C., Mossmann, H. & Rajewsky, K. Deletion of a *DNA polymerase β* gene segment in T cells using cell type-specific gene targeting. *Science* **265,** 103–106 (1994).
13. Zimmerman, L. *et al.* Independent regulatory elements in the *nestin* gene direct transgene expression to neural stem cells or muscle precursors. *Neuron* **12,** 11–24 (1994).
14. Soriano, P. Generalized lacZ expression with the *ROSA26* Cre reporter strain. *Nature Genet.* **21,** 70–71 (1999).
15. Dunwoodie, S. L., Henrique, D., Harrison, S. M. & Beddington, R. S. P. Mouse *Dll3*: a novel divergent *Delta* gene which may complement the function of other *Delta* homologues during early pattern formation in the mouse embryo. *Development* **124,** 3065–3076 (1997).
16. Campos, L. S., Duarte, A. J., Branco, T. & Herique, D. *mDll1* and *mDll3* expression in the developing mouse brain: role in the establishment of the early cortex. *J. Neurosci. Res.* **64,** 590–598 (2001).
17. Ohtsuka, T. *et al. Hes1* and *Hes5* as Notch effectors in mammalian neuronal differentiation. *EMBO J.* **18,** 2196–2207 (1999).
18. Kuhlbrodt, K., Herbarth, B., Sock, E., Hermans-Borgmeyer, I. & Wegner, M. Sox10, a novel transcriptional modulator in glial cells. *J. Neurosci.* **18,** 237–250 (1998).
19. Lu, Q. R. *et al.* Sonic hedgehog-regulated oligodendrocyte lineage genes encoding bHLH proteins in the mammalian central nervous system. *Neuron* **25,** 317–329 (2000).
20. Zhou, Q., Wang, S. & Anderson, D. J. Identification of a novel family of oligodendrocyte lineage-specific basic helix-loop-helix transcription factors. *Neuron* **25,** 331–343 (2000).
21. Takebayashi, H. *et al.* Dynamic expression of basic helix-loop-helix Olig family members: implication of Olig2 in neuron and oligodendrocyte differentiation and identification of a new member, Olig3. *Mech. Dev.* **99,** 143–148 (2000).
22. Mizuguchi, R. *et al.* Combinatorial roles of olig2 and neurogenin2 in the coordinated induction of pan-neuronal and subtype-specific properties of motoneurons. *Neuron* **31,** 757–771 (2001).
23. Novitch, B. G., Chen, A. I. & Jessell, T. M. Coordinate regulation of motor neuron subtype identity and pan-neuronal properties by the bHLH repressor Olig2. *Neuron* **31,** 773–789 (2001).
24. Pfaff, S. L., Mendelsohn, M., Stewart, C. L., Edlund, T. & Jessell, T. M. Requirement for LIM homeobox gene *Isl1* in motor neuron generation reveals a motor neuron-dependent step in interneuron differentiation. *Cell* **84,** 309–320 (1996).
25. Chenn, A. & McConnell, S. K. Cleavage orientation and the asymmetric inheritance of Notch1 immunoreactivity in mammalian neurogenesis. *Cell* **82,** 631–641 (1995).
26. Qian, X., Goderie, S. K., Shen, Q., Stern, J. H. & Temple, S. Intrinsic programs of patterned cell lineages in isolated vertebrate CNS ventricular zone cells. *Development* **125,** 3143–3152 (1998).
27. Noctor, S. C., Flint, A. C., Weissman, T. A., Dammerman, R. S. & Kriegstein, A. R. Neurons derived from radial glial cells establish radial units in neocortex. *Nature* **409,** 714–720 (2001).
28. Cayouette, M., Whitmore, A. V., Jeffery, G. & Raff, M. Asymmetric segregation of Numb in retinal development and the influence of the pigmented epithelium. *J. Neurosci.* **21,** 5643–5651 (2001).
29. Zhong, W., Mirkovitch, J. & Darnell, J. E. Jr Tissue specific regulation of mouse *hepatocyte nuclear factor 4* expression. *Mol. Cell. Biol.* **14,** 7276–7284 (1994).

Acknowledgements We thank members of the Zhong laboratory for discussions, C. Jacobs and H. Keshishian for comments, K. Jakobsdottir for support (P.H.P.), J. Zhang for technical assistance, Developmental Studies Hybridoma Bank, D. Anderson, R. Kageyama, U. Lendahl, M. Lewandoski, M. Nakafuku, H. Takebayashi and M. Wegner for reagents. K.Z. is supported by a Yale Anderson fellowship. Y.N.J. is a HHMI investigator. This work was supported by a Yale Hellman Family fellowship and grants from March of Dimes and NINDS to W.Z. and from NIMH to the Silvio Conte Center for Neuroscience Research at UCSF.

Competing interests statement The authors declare that they have no competing financial interests.

Correspondence and requests for materials should be addressed to W.Z. (e-mail: weimin.zhong@yale.edu).

N-CoR controls differentiation of neural stem cells into astrocytes

Ola Hermanson*†, Kristen Jepsen* & Michael G. Rosenfeld*

** Howard Hughes Medical Institute, Department of Molecular Medicine, University of California, San Diego, School of Medicine, 9500 Gilman Drive, Room 345, La Jolla, California 92093-0648, USA*

Understanding the gene programmes that regulate maintenance and differentiation of neural stem cells is a central question in stem cell biology. Virtually all neural stem cells maintain an undifferentiated state and the capacity to self-renew in response to fibroblast growth factor-2 (FGF2)[1–5]. Here we report that a repressor of transcription, the nuclear receptor co-repressor (N-CoR), is a principal regulator in neural stem cells, as FGF2-treated embryonic cortical progenitors from *N-CoR* gene-disrupted mice display impaired self-renewal and spontaneous differentiation into astroglia-like cells. Stimulation of wild-type neural stem cells with ciliary neurotrophic factor (CNTF), a differentiation-inducing cytokine[3], results in phosphatidylinositol-3-OH kinase/Akt1 kinase-dependent phosphorylation of N-CoR, and causes a temporally correlated redistribution of N-CoR to the cytoplasm. We find that this is a critical strategy for cytokine-induced astroglia differentiation and lineage-characteristic gene expression. Recruitment of protein phosphatase-1 to a specific binding site on N-CoR exerts a reciprocal effect on the cellular localization of N-CoR. We propose that repression by N-CoR, modulated by opposing enzymatic activities, is a critical mechanism in neural stem cells that underlies the inhibition of glial differentiation.

N-CoR was initially defined as a regulator of nuclear receptor-mediated repression[6], but has been shown to interact with and act as a co-repressor for many other transcription factors including CBF1 (suppressor of hairless, Lag-1, CSL, RBP-Jκ)[7], which acts downstream of the transmembrane receptor notch[8]. Notch signalling has long been implicated in the inhibition of neuronal differentiation, and FGF2-mediated maintenance of notch expression and responsiveness may be one characteristic of the neural stem cell[8–10]; however, *in vivo* evidence for a role of N-CoR in this context is lacking. N-CoR protein levels are high in undifferentiated, proliferating neural progenitors located in the ventricular zones of the embryonic brain[11] (Fig. 1a, and data not shown). Previous evaluation of *N-CoR* gene-deleted mice ($N\text{-}CoR^{-/-}$), which generally die before embryonic day 16 (E16)[11], revealed that neural induction and early development proceed grossly normal through to E12.5 in the absence of N-CoR. However, the brains of $N\text{-}CoR^{-/-}$ mice show progressively more severe aberrations beginning at E14.5, including

† Present address: Department of Cell and Molecular Biology, Medical Nobel Institute, Karolinska Institute, SE-171 77 Stockholm, Sweden